Amphiphilic Polymer Nanoparticles: Characterization and Assessment as New Drug Carriers

Pranabesh Dutta, Saurabh Shrivastava, Joykrishna Dey*

An amino-acid-based hydrophobically modified biocompatible copolymer, poly[(sodium *N*-acryloyl-L-valinate)-*co*-(*N*-octylacrylamide)] was synthesized and characterized. Techniques such as fluorescence probes, DLS, and TEM were used to investigate its aggregation behavior in aqueous solution. The copolymer was observed to form micellar aggregates having diameters in the nanometer range in aqueous solution (pH = 8) through inter-chain hydrophobic association. This behavior was found to be similar to that of poly[(sodium *N*-acryloyl-L-valinate)-*co*-(*N*-dodecylacrylamide)]. The compact micellar nanostructures were observed to be stable with respect to changes of pH and temperature. The encapsulation and release of griseofulvin, a hydrophobic model drug, was studied.

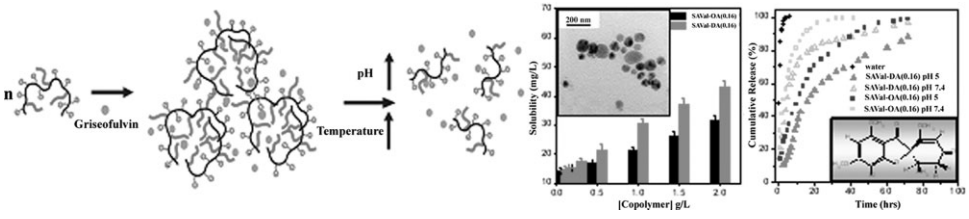

Introduction

The drugs that are discovered and developed to market by pharmaceutical companies are found to be mostly hydrophobic in nature. When administered to the body as such, they are often precipitated and degraded in the blood stream without reaching the target zone, and thus cause severe side effects. The poor solubility of these hydrophobic molecules, therefore, poses a major problem to the drug industry in drug formulation, and thus limits their possible application in drug delivery.[1] In order to reduce these drawbacks and prevent toxic side effects, various drug delivery systems such as biodegradable microparticles, microcapsules, lipoproteins, and liposomes have been developed.[2,3] Micelles made up of surfactants and polymers are very effective in this regard. The hydrophobic core of these micelles is protected by the hydrophilic peripheries. A large number of poorly soluble hydrophobic drugs can be solubilized into the hydrophobic core and hence bioavailability of the drug can be enhanced. Although the micelles formed by the low-molecular-weight surfactants are routinely used in the pharmaceutical industry, they break up in milliseconds on dilution with body fluids resulting in burst release. Since application of micelles as drug carriers mainly depends on their stability and morphology, it is therefore important to seek micelles with a stable structure of well-defined sizes (usually 20–200 nm).[4] This has led researchers to consider micelle-forming amphiphilic polymers as alternatives. Like low-molecular-weight surfactants, amphiphilic polymers also associate in water to form "polymeric micelles" consisting of a hydrophobic core stabilized by a corona of hydrophilic moieties that are exposed towards the aqueous environment. In contrast to micelles of low-molecular-weight surfactants, polymeric micelles may remain kinetically stable on dilution and dissociate very slowly. The dissociation time may be several hours to days, which is due to the low ($\approx 10^{-6}$ M) or zero critical aggregation concentration (CAC), and allows the drug to be protected more effectively within the dense core.

P. Dutta, S. Shrivastava, J. Dey
Department of Chemistry, Indian Institute of Technology, Kharagpur 721302, India
Fax: +91 3222 25 5303; E-mail: joydey@chem.iitkgp.ernet.in

DOI: 10.1002/mabi.200900135

As a result, interest has grown in polymeric nanoparticles of different categories. Several studies have been performed over the past few years with micelle-forming block copolymers. Most of these have been conducted on poly(ethylene oxide) (PEO)/poly(propylene oxide) (PPO) triblock copolymers (pluronics).[5–7] Various hydrophobic drugs including haloperidol,[8] indomethacin,[9] epirubicin,[10] doxorubicin (DOX),[10] and amphotericin B[11] have been successfully loaded into the micellar compartments of these copolymers. Some of these have been used in clinical trials. Beside pluronics, various other block copolymer systems have also been explored. Reviews available in the literature have discussed the advantages and disadvantages of theses polymeric systems in view of their pharmaceutical applications.[12–14]

However, the difficulty and high cost of preparation of block copolymers sometimes become disadvantageous in their industrial formulation, and this has prompted researchers to consider other micelle-forming polymers. The micelles made of hydrophobically modified polymers (HMPs) can also be regarded as potential drug reservoirs from which drug molecules can be delivered over a longer period of time. Unlike block copolymers, they do not display any specific CAC values, but rather form micelles through hydrophobic interaction within a single polymer chain (intra-molecular association) or between different polymer chains (inter-molecular association).[15–17] Depending on the chemical structures these are known to form different types of micellar aggregates, such as unimer micelles, unicore multipolymer micelles, and polycore multipolymer micelles.[18,19] Since hydrophobic chains in such types of micelles are more tightly packed and less mobile in contrast to low-molecular-weight surfactants, these are very stable to dilution. The stability of the micelles further depends on the nature of the hydrophobes and hydrophiles. Depending on the nature of the hydrophilic groups, they can also exhibit conformational transition by external factors such as pH or ionic strength. The micelles formed by this type of copolymer have been shown to dissolve various hydrophobic compounds in aqueous solution.[20,21] A substrate solubilized into the micelle can subsequently be released either by a simple thermodynamic equilibrium with the medium or by a drastic change of the external conditions, such as pH or temperature. All the structural characteristics highlighted above therefore suggest that such a micelle type could be considered as a competent drug delivery vehicle. However, to the best of our knowledge, very few bio-relevant HMPs have been explored so far.[22,23]

Considering the prospective applications of these systems in the pharmaceutical industry, we recently investigated and reported the aggregation behavior of the copolymer, poly[(sodium *N*-acryloyl-L-valinate)-*co*-(*N*-dodecylacrylamide)] [SAVal-DA(0.16)].[24] It has been observed that SAVal-DA(0.16) undergoes self-association above a CAC (9×10^{-4} g · L^{-1}) to form multipolymer unicore micelles. In this work, we synthesized a structurally similar amino acid-based HMP, poly[(sodium *N*-acryloyl-L-valinate)-*co*-(*N*-octylacrylamide)] [SAVal-OA(0.16)], keeping the hydrophobe concentration fixed at 16 mol-% (Scheme 1). Owing to the net negative charge (due to carboxylate groups), these copolymers are expected to be biologically active.[25] Since the copolymers in solution form micelle-like structures through inter-chain association, they are expected to solubilize and deliver hydrophobic drugs over a period of time in the physiological ranges of pH and temperature. Also, as seen from the chemical structures, the copolymers possess both the acrylamide and isopropyl functionalities similar to poly(*N*-isopropylacrylamide), p(NIPAM). Thus, it is expected that they may exhibit thermoresponsive behaviors similar to p(NIPAM). Therefore, the main aims of our work were:

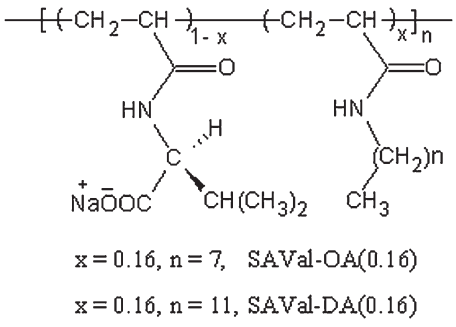

Scheme 1. Chemical structures of copolymers.

1. To compare the self-assembly behaviors of copolymer SAVal-OA(0.16) with the longer hydrophobic chain analog SAVal-DA(0.16) in aqueous solution.
2. To investigate the microenvironment of the micellar aggregates.
3. To study the effect of pH and temperature on the copolymer aggregates in aqueous solution.
4. To estimate the drug solubilization capacity of both copolymers at different values of solution pH. To study drug release kinetics upon change of solution pH and temperature.

Experimental Part

Materials

The fluorescence probes like pyrene, 1,6-diphenyl-1,3,5-hexatriene (DPH), and *N*-phenyl-1-naphthylamine (NPN) (Aldrich) were recrystallized from ethanol or acetone–ethanol mixture at least three times before use. The hydrophobic drug, griseofulvin, was purchased from Sigma-Aldrich and used as received. All the reagents and solvents, particularly *N,N*-dimethylformamide (DMF), ethanol, methanol, tetrahydrofuran (THF), acetone, and dichloromethane, were of good commercial quality and were dried

and distilled fresh before use. Sodium chloride, potassium chloride, sodium dihydrogen phosphate, and sodium hydroxide were of analytical grade and were procured from SRL, Mumbai. Double distilled water was used for preparation of all solutions.

Synthesis of Copolymer

Copolymer SAVal-OA(0.16) was prepared with the monomer sodium *N*-acryloyl-L-valinate (SAVal) and *N*-octylacrylamide (OA) in DMF at 60 °C using azoisobutyronitrile (AIBN) as a radical initiator in the same manner as reported for SAVal-DA(0.16).[24] Briefly, sodium *N*-acryloyl-L-valinate (SAVal) (3.0 g, 0.021 mol) and *N*-octylacrylamide (OA) (0.76 g, 0.0042 mol) were dissolved in DMF. Dry oxygen-free nitrogen was purged through the solution for 45 min at 60 °C followed by addition of AIBN (1 mol-% of the total monomer concentration). The polymerization was continued for 24 h and the product was recovered by precipitation with a large excess of acetone. Purification was achieved by repeated reprecipitation from methanol with acetone and the product was dissolved in pure water. Subsequently, the solution was dialyzed (molecular-weight cutoff ≈12 000–14 000) against distilled water (pH = 8–9) for 1 week and then lyophilized.

Methods

The UV-visible spectra were recorded with a Shimadzu (model 1601) spectrophotometer. The optical rotation was measured with Jasco P-1020 digital polarimeter. Melting points were determined with an Instind (Kolkata) melting point apparatus in open capillaries. The pH measurements were taken with a digital pH meter Model pH 5652 (EC India Ltd., Kolkata) using a glass electrode.

Gel permeation chromatography (GPC) was used to determine the molecular weight and molecular weight distribution of the copolymers. GPC analysis was performed at 70 °C on a Spectra Physics instrument equipped with a Shodex RI-101 refractometer detector and two 300-mm columns. Narrow polydispersity polystyrene standards were used as calibration standards. DMF was used as eluent at a flow rate of 0.8 mL · min^{-1}.

The steady-state fluorescence spectra of pyrene and NPN were measured with a SPEX Fluorolog-3 spectrofluorometer. The pyrene solutions were excited at 335 nm and the emission intensity was recorded in the wavelength range 350–500 nm. The samples containing NPN were excited at 340 nm and emission was collected in the range 360–550 nm. Stock solutions of pyrene and NPN were prepared by adding the compound to buffer solution and agitating the mixture with magnetic stirring for 24 h. The excess compound was removed by centrifugation followed by filtration through a Millipore syringe filter (0.22 μm) to obtain probe-saturated solution.

Steady-state fluorescence anisotropy (r) was measured on a Perkin Elmer LS-55 spectrophotometer equipped with a thermostatted cell holder and polarizing filters that used the L-format configuration. DPH was used as the fluorescent probe. The concentration of DPH was adjusted to 2×10^{-7} M by adding the appropriate amount of ethanol stock solution of the probe. The excitation wavelength was set at 350 nm and the emission was monitored at 450 nm. The temperature of the samples was controlled using the water-jacketed magnetically stirred cell holder in the spectrometer connected to a Thermo Neslab RTE-7 circulating water bath that gave temperature control within ±0.1 °C. Temperature-dependent fluorescence measurements were performed in the range of 20–60 °C with an increment of 5 °C. Before every measurement, the solution was equilibrated at the desired temperature for at least 10 min.

Fluorescence lifetimes were determined from time-resolved intensity decays by time-correlated single-photon counting using a picosecond diode laser at $\lambda = 370$ nm (IBH, UK, nanoLED-07) as the light source for excitation. The decay kinetics of DPH was recorded at the emission wavelength of 460 nm. The decays were analyzed using IBH DAS-6 decay analysis software.

Transmission electron microscopy (TEM) images of copolymer solutions were taken with a JEOL-JEM 2100 (Japan) electron microscope operating at an accelerating voltage of 200 kV at room temperature. The specimen was prepared by immersing a 400-mesh carbon-coated copper grid into the copolymer solution (1 g · L^{-1}) for 1 min, blotting to remove excess liquid, and drying in a desiccator.

Dynamic light scattering (DLS) experiments were carried out on a Zetasizer Nano ZS (Malvern Instrument Laboratory, Malvern, UK) optical system equipped with a He-Ne laser operated at 4 mW ($\lambda_0 = 632.8$ nm), and a digital correlator. The scattering intensity was measured at an angle of 173° to the incident beam. Prior to the measurements, each solution was cleaned by centrifuging at a speed of 5 000 rpm for 15 min followed by filtration through a 0.45-μm filter paper (Millipore Millex syringe filter). The final solution was loaded into an optical-quality cylindrical quartz sample cell. The sample cell was placed in the DLS optical system for 30 min to equilibrate at the desired temperature (25–60 °C). The data acquisition was carried out for 2 min and each experiment was repeated at least twice. The apparent diffusion coefficient (D_{app}) was calculated by cumulant analysis (first order) of an autocorrelation function generated by the scattered light intensity fluctuations. The average hydrodynamic diameter (d_h) was calculated from diffusion coefficients using the Stokes-Einstein equation:

$$D_{app} = k_B T / 3\pi\eta d_h \quad (1)$$

where k_B is the Boltzmann constant, T is the absolute temperature, and η is the viscosity of the solvent.

Encapsulation Experiments

Aqueous solubilization measurements were carried out to estimate the ability of the copolymer to solubilize water-insoluble nonpolar compounds in its hydrophobic domain. A poorly soluble (≈10 mg · L^{-1} at 25 °C)[26] aromatic drug, griseofulvin, was used as a model compound to evaluate the solubilization capacity of the micellar solution of the copolymer. To produce fine particles, an excess of griseofulvin (approximately ten times the solubility in water) taken in a small centrifuge tube was dissolved in chloroform and then evaporated by passing N_2 gas through it. A 5-mL polymer solution (≈0.05–2.0 g · L^{-1}) was rapidly added to the tube containing the drug. The mixture was left for 5 days at room temperature with stirring to ensure solubilization equilibrium. Before filtration

Macromolecular Journals
DOI: 10.1002/mabi.200900135

it was allowed to stand for another 24 h. To remove nonsolubilized drug the solution mixture was centrifuged at a speed of 4 000 rpm for 10 min followed by careful filtration using Millipore Millex filter (0.45 μm pore diameter). The samples were diluted with methanol to enable analysis by UV spectroscopy and quantified at a wavelength of 292 nm using the previously recorded calibration curve. The copolymer solution at the same dilution was used as a blank. This procedure was also applied to a solution of griseofulvin equilibrated with water alone to make the necessary corrections for the water solubility of griseofulvin. Measurements were carried out in triplicate, and results were averaged.

Drug Release Kinetics

For *in vitro* drug release experiments, 1 mL of griseofulvin solution in water ($10\ \mu g \cdot mL^{-1}$) or griseofulvin-loaded ($\approx 40–50\ \mu g \cdot mL^{-1}$) polymer micelles ($1\ g \cdot L^{-1}$) was added to a double-sided Biodialyzer (Aldrich) dialysis compartment fitted with membranes with molecular weight cutoff of 12–14 kDa. To remove any untrapped drug, the solution was immersed and dialyzed against 20 mL of buffer solution of pH = 5. After 2 h of dialysis against pH = 5, the dialysis cell was withdrawn and maintained into a freshly prepared buffer solution and dialyzed against buffer of the required pH (pH = 5.0: acetate; pH = 7.4: phosphate, 0.1 M NaCl) at 37 °C. The copolymer concentration was kept at $1\ g \cdot L^{-1}$ in all the release experiments. Aliquots of 2 mL were withdrawn periodically from the solution. The volume of the solution was held constant by adding 2 mL of fresh buffer solution after each sampling to ensure sink conditions. The amount of griseofulvin released from micelles was determined by monitoring the absorbance at a wavelength of 292 nm. The cumulative drug release was calculated as

$$\text{cumulative drug release}\ (\%) = M_t/M_\infty \times 100$$

where M_t is the amount of drug released from micelles at time t, and M_∞ is the amount of drug released from the micelles at time infinity.

Results and Discussion

Molecular Characterization of SAVal-OA(0.16)

The copolymer under investigation was characterized by Fourier-transform infrared (FT-IR) and ^{1}H NMR spectroscopy. The absence of the −C=C− bond-stretching frequency at $1\,600\ cm^{-1}$ in the FT-IR spectrum (not shown) suggested formation of a polymeric structure of the acrylamide monomers. A polymeric structure was further confirmed by the disappearance of the vinylic proton signal at $\delta = 5–6$ in the ^{1}H NMR spectrum (not shown). To determine the chemical composition of the copolymer, the monomer peaks in the ^{1}H NMR spectrum were integrated for comparison. However, due to the overlapping broad bands in the ^{1}H NMR spectrum, we were unable to determine the exact monomer composition in the final copolymer. Despite this, we note that Kawata et al.[27] have demonstrated that the copolymer compositions of structurally similar HMPs are equal to the feed composition. Hence, in this work we also assumed that the copolymer composition of the polymer was virtually the same as the composition in the monomer feed. This implies that the reactivity ratios of the monomers are equal to 1.0. In other words, these HMPs are statistical copolymers. In fact, in radical polymerization, one would seldom experience an instance of block copolymer formation. Although in most cases, formation of alternating copolymers is favored, one still finds limited instances of copolymerization approaching ideal behavior.

The number-average molar mass ($\overline{M}_n$) of the copolymer SAVal-OA(0.16), as determined by size exclusion chromatography, was 1.18×10^6 with a polydispersity index (PDI) of 1.21. The molecular weight of the copolymer thus obtained is quite close to that of SAVal-DA(0.16) ($\overline{M}_n \approx 1.17 \times 10^6$, PDI = 1.15).[24] Given that is the HMPs have almost equal chain lengths, the aggregation behaviors of the HMPs in an aqueous medium are expected to be similar.

Self-Assembly Studies with SAVal-OA(0.16)

The self-aggregation of copolymer SAVal-OA(0.16) was investigated by use of a fluorescence probe technique using NPN and pyrene as the probe molecules. As reported elsewhere,[24,28] NPN is a hydrophobic fluorescent probe with spectral properties that depend on the environment of the system. Usually, a very weak fluorescence is detected in an aqueous medium with an emission maximum (λ_{max}) at 460 nm. This maximum undergoes a blue shift and increases markedly in intensity in going from water to a less polar solvent. On the other hand, the intensity ratio (I_1/I_3) of the first to third vibronic band of pyrene is dependent on the polarity of the environment and it decreases in going from polar to non-polar media.[29] Therefore, the fluorescence spectra of both NPN and pyrene were measured in the presence of different polymer concentrations. The emission maximum of NPN undergoes a blue shift accompanied by a huge rise in fluorescence intensity in the presence of copolymer, indicating partitioning of NPN into the hydrophobic domains. The shift of emission maximum ($\lambda_{water} - \lambda_{poly}$) determined at different polymer concentrations is plotted in Figure 1. Both the relative fluorescence intensity (I/I_0) (see inset of Figure 1), and $\Delta\lambda$ were found to increase with increased polymer concentration. In the same figure, the I_1/I_3 ratio of the pyrene fluorescence spectrum is plotted against polymer concentration. As can be seen in Figure 1, there is no appreciable change in $\Delta\lambda$ or I_1/I_3 ratio at concentration well below $2.2 \times 10^{-2}\ g \cdot L^{-1}$. However, with the increase in polymer concentration, the value of $\Delta\lambda$ gradually increased and the I_1/I_3 ratio gradually decreased, reaching a plateau at $[\text{SAVal-OA(0.16)}] > 1.0\ g \cdot L^{-1}$. The concentration corresponding to the inflection point of the plots as indicated in

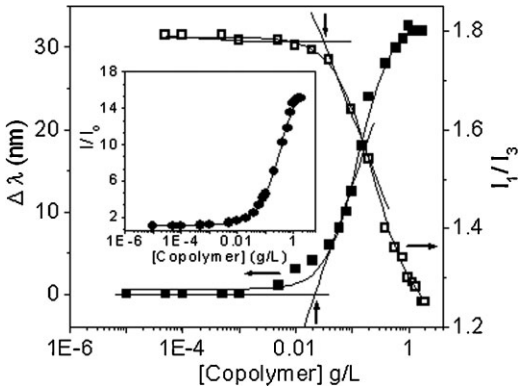

Figure 1. Plots of shift of emission maximum ($\Delta\lambda = \lambda_{water} - \lambda_{poly}$) of NPN (■) and intensity ratio (I_1/I_3) of pyrene (□) versus SAVal-OA(0.16) concentration at 30 °C. Inset: plot of relative fluorescence intensity (I/I_o) of NPN at different polymer concentration.

Figure 1 was taken as the CAC. The CAC value (see Table 1) thus obtained is almost 25 times higher than that for SAVal-DA(0.16), which contains a dodecyl chain as the hydrophobic unit. This suggests that inter-polymer association occurs through strong hydrophobic interactions of the hydrophobic units.

The microenvironments of the copolymer aggregates thus formed are expected to be nonpolar, rigid, and compact compared to the micelles of common surfactants. Indeed, the values of $\Delta\lambda$ and I_1/I_3 ratio presented in Table 1 suggest that the polarity of the microenvironments of the aggregates is much less than that of water. For comparison purposes, Table 1 shows the corresponding properties of the copolymer SAVal-DA(0.16).[24] It is observed that the micropolarity parameter in the case of SAVal-OA(0.16) is higher than that of SAVal-DA(0.16). This is due to enhanced polymer chain entanglement as a result of the relatively stronger hydrophobic interaction among dodecyl chains of SAVal-DA(0.16). This should make the microenvironment of the copolymer aggregate more rigid. The rigidity of the microenvironments was therefore estimated by measuring the steady-state fluorescence anisotropy (r)

Table 1. Critical aggregation concentration (CAC), polarity parameters ($\Delta\lambda$ and I_1/I_3), and microviscosity (η_m) for 1.0 g · L^{-1} SAVal-OA(0.16) and SAVal-DA(0.16) in aqueous phosphate buffer solution (pH = 8).

Copolymer	CAC × 10^4	Δλ	I_1/I_3	η_m
	g · L^{-1}	nm		mPa · s
SAVal-OA(0.16)	220	32.0	1.34	73.6
SAVal-DA(0.16)[a)]	9.0	37.0	1.02	87.8

[a)]Data for SAVal-DA(0.16) was taken from Dutta et al.[24]

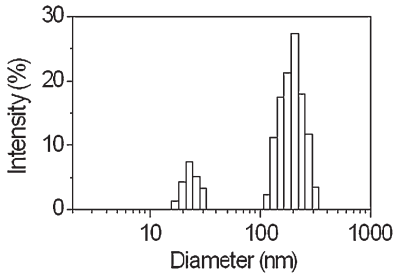

Figure 2. Size distributions of the aggregates in 1.0 g · L^{-1} aqueous buffer solution (pH = 8) of SAVal-OA(0.16) at 25 °C.

and fluorescence lifetime (τ_f) of the probe (DPH) at a polymer concentration of 1.0 g · L^{-1}. These data were used to calculate the microviscosity (η_m) according to the procedure reported in the literature.[30] The η_m value (Table 1) thus obtained is found to be lower than that of SAVal-DA(0.16) copolymer. This is consistent with the micropolarity of the aggregates.

The results of fluorescence probe studies indicate that the aggregates of SAVal-OA(0.16) are less compact relative to those of SAVal-DA(0.16) copolymer. This is also supported by the results of DLS measurements. The DLS experiments were performed to measure the hydrodynamic diameter of the aggregates formed by the copolymer in aqueous buffer solution. The intensity-averaged size distributions of the aggregates in 1.0 g · L^{-1} SAVal-OA(0.16) solution at 25 °C are presented in Figure 2. The copolymer exhibited a bimodal distribution with peaks appearing at 25 nm and 210 nm. In contrast, a broad distribution (not shown here) with mean diameter of 80 nm was observed for SAVal-DA(0.16) copolymer.[24]

In order to investigate the shape of the aggregates formed in aqueous solution by the copolymer, we took TEM images of the copolymer solution. The micrograph taken for 1.0 g · L^{-1} copolymer solution is presented in Figure 3. The TEM picture clearly shows near-spherical aggregates of

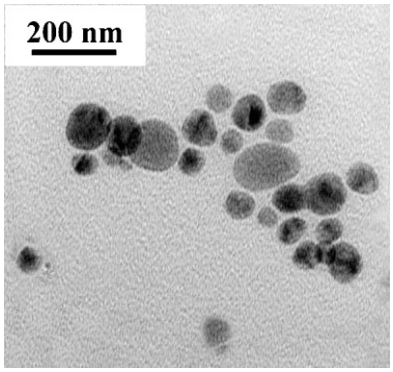

Figure 3. TEM picture (unstained) of 1.0 g · L^{-1} SAVal-OA(0.16) solution.

Macromol. Biosci. **2009**, *9*, 1116–1126

Macromolecular Journals

DOI: 10.1002/mabi.200900135

different sizes in the range 50–150 nm. The sizes of the polymer nanoparticles are consistent with those obtained from DLS measurements. As indicated earlier, the molecular weight of the copolymer is very high. Therefore, in concentrated aqueous solutions, such large polymer chains would entangle with each other through hydrophobic interaction of the hydrophobes to form a globular aggregate. In such cases, the diameter of the aggregates, unlike surfactant micelles, is expected to be much higher than twice the hydrophobe chain length. The spheroidal aggregates, as shown in the TEM picture, could be easily mistaken as disk-like aggregates. Although the formation of disk-shaped micelles and bilayer vesicles by other copolymers[31] has been reported in the literature, such a possibility can be eliminated based on the structure of the large copolymers with only 16% hydrophobe content. Since disk-like micelles have a bilayer structure, the membrane rigidity would be much higher. However, fluorescence probe studies have suggested that the microenvironments of the probes (NPN, pyrene, and DPH) are spherical or rod-shaped micelles. In the case of disk-like aggregates, one would normally find micropolarity and microviscosity to be respectively on the higher and lower side as the probe molecules would be more exposed to bulk water. Also, disk-like micelles would produce rod-like aggregates through stacking, which are not revealed in the TEM image in Figure 3. Therefore, it is believed that the aggregates formed by the copolymers were spherical or spheroidal micelles.

Effect of pH

Due to the presence of carboxylate groups on the macromolecular chain, the polymer was expected to exhibit pH-dependent aggregation. This was investigated by a fluorescence probe method. Figure 4 illustrates the variation of I/I_0 and $\Delta\lambda$ of NPN probe with the solution pH at a given concentration of both SAVal-OA(0.16) and SAVal-DA(0.16) copolymers. The pH effect was studied with 0.25 g · L^{-1} polymer solution in order to avoid precipitation at low pH. For both polymers, $\Delta\lambda$ as well as I/I_0 increased steadily with the decrease of pH. At low pH (≈5), the carboxylate groups along the polymer backbone become partially protonated, which reduces ionic repulsions among them. Consequently, the polymer collapses into a compact aggregate due to the loss of ionic character. This imparts higher hydrophobicity to the microdomains resulting in an increase of $\Delta\lambda$ and I/I_0. At alkaline pH (≈8), the polymer coil expands and allows water molecules to penetrate into the micelle, which increases the polarity of the microenvironment. This means that the partition coefficient of NPN decreases when the pH is increased. Therefore, if required, hydrophobic drug molecules can be encapsulated into the

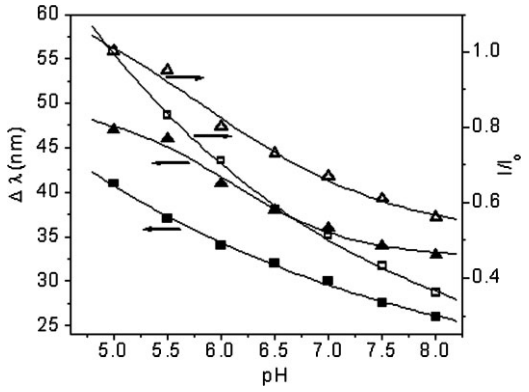

Figure 4. Plot of $\Delta\lambda$ (solid symbols) and I/I_0 (open symbols) of NPN probe as a function of pH in the presence of 0.25 g · L^{-1} copolymer solution at 30 °C: (■), (□) SAVal-OA(0.16), and (▲), (△) SAVal-DA(0.16).

hydrophobic compartments formed by the copolymer chains at low pH, and can subsequently be released at higher pH.

In order to investigate the conformational changes of the copolymers, DLS measurements were further performed at two different pH values. The intensity average size distributions in 0.25 g · L^{-1} solution of both copolymers at pH = 5.0 and 8.0 are presented in Figure 5. It is observed that both copolymers exhibit bimodal size distributions at pH = 8.0, which can be attributed to two different types of micellar aggregates formed by the inter-chain association of the hydrophobic units. Upon decreasing the solution pH, the carboxylate groups get progressively neutralized and favor stronger hydrophobic interaction, which means more compact aggregates are formed. In fact, decrease of pH can also induce formation of smaller aggregates through intra-

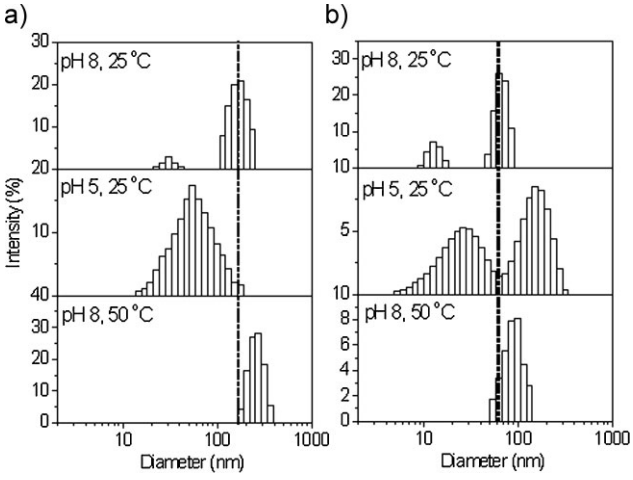

Figure 5. Intensity average size distributions for 0.25 g · L^{-1} polymer solution of (a) SAVal-OA(0.16), and (b) SAVal-DA(0.16) at pH = 8.0 and 5.0 at 25 °C and 50 °C.

chain association of the hydrophobe units. This causes widening of the distributions as manifested by the merger of the bimodal distributions into one in the case of SAVal-OA(0.16) with concomitant decrease of the apparent hydrodynamic diameter. However, with the SAVal-DA(0.16) copolymer, both distributions shift toward larger diameter. This is because upon decreasing the degree of ionization, electrostatic repulsion among micellar aggregates is reduced and allows them to come into close proximity and fuse to form polycore multipolymer micelles, which results in an increase of average diameter. The polycore multipolymer micelle formation becomes facilitated at higher polymer concentrations.

Thermal Stability of the Copolymer Micelles

The thermal response of the copolymer micelles was investigated by a fluorescence probe technique using both NPN and DPH probes. As discussed earlier, the fluorescence intensity and emission maximum of NPN change substantially in going from a hydrophobic environment, such as the core of the micelles, to bulk water. The fluorescence emission spectra of NPN were therefore recorded in aqueous buffer solution (pH = 7.4) in the presence of 0.25 $g \cdot L^{-1}$ copolymer at various temperatures. The noticeable large fluorescence intensity at temperature below 30 °C was due to the enhanced solubilization of NPN in the hydrophobic domains of the aggregates. When the temperature was raised above 30 °C, the fluorescence intensity gradually decreased and the position of the emission maximum underwent a red shift, which suggests disintegration of the micellar aggregates to individual polymer chains, and thus release of the NPN molecules. This is shown in the plots of I/I_0 and $\Delta\lambda$ as a function of temperature (Figure 6a). The decrease of $\Delta\lambda$ value clearly suggests that the polarity of the microdomains increased as a result of polymer chain dissociation. This is supported by the decrease of fluorescence anisotropy of DPH probe with the increase of temperature. The plots of fluorescence anisotropy (r) of DPH as a function of temperature in solution containing 0.25 $g \cdot L^{-1}$ copolymer are presented in Figure 6b. The decrease of r suggests that as the temperature was increased the microenvironments of the aggregates became less viscous. It is important to note that when the solution temperature was gradually lowered to 20 °C from higher temperature, the fluorescence intensity of NPN increased and the emission maxima underwent a blue shift (not shown here), demonstrating the thermoreversible aggregation.

For both copolymers, I/I_0, $\Delta\lambda$, and the value of r decreased with the increase in temperature, although it should be noted that the change observed for SAVal-DA(0.16) is relatively less in comparison with SAVal-OA(0.16). This suggests that the nanoparticles of SAVal-DA(0.16) copolymer were much more stable than the less hydrophobic chain analog. When similar studies were carried out using 1.0 $g \cdot L^{-1}$ polymer solution, the fluorescence intensity of NPN decreased with the increase in temperature, but neither $\Delta\lambda$ nor r changed with the temperature (see Figure 6). This indicates that the microenvironment of the probes remained unchanged when the solution was heated. As discussed earlier, in concentrated solutions, both copolymers exist as polycore multipolymer micelles, which gradually dissociate to individual unicore multipolymer micelles with the rise of temperature. Consequently the probe molecules that were solubilized within the interstices of the polycore micelles became free, causing decreased fluorescence intensity of the NPN probe. To support the results of fluorescence probe studies, the thermal stability of the copolymer micelles was also examined at two different concentrations (0.25 and 1.0 $g \cdot L^{-1}$) for both copolymers by DLS. As shown in Figure 5, copolymer SAVal-DA(0.16) at lower concentration revealed a bimodal size distribution at a measurement temperature of 25 °C with a peak around 20 nm and another peak corresponded to a larger aggregate at 220 nm. However, when the solution was heated to 50 °C, the small peak corresponding to the smaller aggregates disappeared and the mean hydrodynamic diameter (d_h) assigned to the larger aggregate increased. A similar trend was also observed with the SAVal-OA(0.16) copolymer at lower concentration. However, the increase in the hydrodynamic diameter at higher temperature was less for SAVal-DA(0.16) copolymer, which suggests that the copolymer with the longer hydrophobic group associated

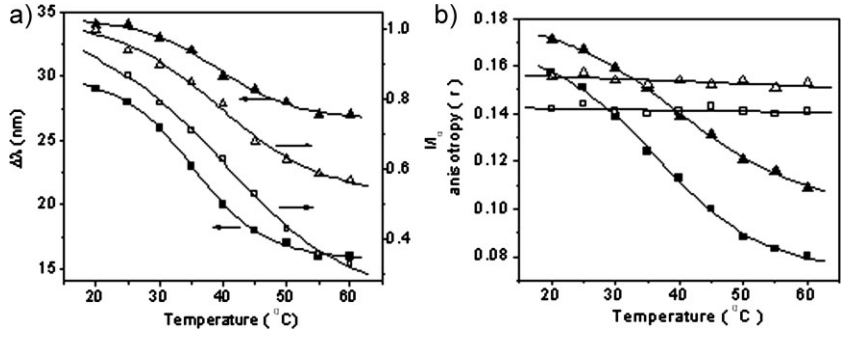

Figure 6. (a) Plot of $\Delta\lambda$ (solid symbols) and I/I_o (open symbols) of NPN versus temperature for 0.25 $g \cdot L^{-1}$ solutions (pH = 7.4) of SAVal-DA(0.16) (triangles) and SAVal-OA(0.16) (squares). (b) Plot of fluorescence anisotropy of DPH versus temperature for 0.25 $g \cdot L^{-1}$ solutions of SAVal-DA(0.16) (▲) and SAVal-OA(0.16) (■), and 1.0 $g \cdot L^{-1}$ solutions of SAVal-DA(0.16) (△) and SAVal-OA(0.16) (□).

Macromolecular Journals
DOI: 10.1002/mabi.200900135

more strongly. It is interesting to observe that the hydrodynamic sizes of the copolymer aggregates at higher concentration ($\approx$1.0 g · L^{-1}) remained almost invariable over the whole temperature range for both copolymers under study. This is consistent with the variation of fluorescence anisotropy of DPH probe with solution temperature (Figure 6). In dilute solution, the micelles were less tightly packed as evident from their larger hydrodynamic diameter. Essentially, the energy provided by heating was enough to weaken the hydrophobic interaction and cause dissociation of the polymer chains. Since the larger aggregate at high concentration corresponds to secondary association of individual micelles (associated unicore micelles),[19] they are more compact and stable and do not undergo any change in their association properties in the range of the heating cycle.

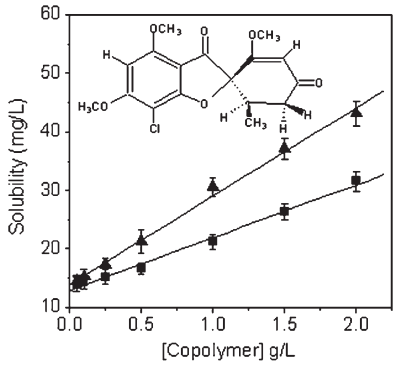

Figure 7. Solubility profiles of griseofulvin with increasing concentration of copolymers in aqueous buffer solution (pH = 7.4) for SAVal-OA(0.16) (■) and SAVal-DA(0.16) (▲). Inset: chemical structure of griseofulvin.

Encapsulation Studies

In order to establish the applicability of the copolymers as drug carriers, encapsulation experiments were carried out employing griseofulvin as a model compound. Griseofulvin (see Figure 7 for structure) is an important antifungal drug often used for the treatment of tinea capitis in children.[32] Owing to its poor aqueous solubility, development of griseofulvin formulations for clinical applications has proven difficult. To improve the bioavailability, different formulations, including solid dispersions,[33] incorporation into liposomes,[34] and associations with bioadhesive polymers,[35] have been adopted. In this study, encapsulation of the drug into the micellar aggregates of the copolymers was achieved by the direct dissolution method in the concentration range 0.05–2.0 g · L^{-1}. The amount of drug loaded at equilibrium was determined spectrophotometrically at a wavelength of 292 nm. The solubility determined at different polymer concentration is plotted in Figure 7. For both copolymers, the solubility increased linearly with concentration. The increase of polymer concentration results in formation of more multipolymer unicore micelles that encapsulate the griseofulvin molecules.

To further evaluate the efficacy of the system in encapsulation, two important parameters, solubilization capacity (S_{cp}) and encapsulation efficiency (E_{ef}) (i.e., the percentage of drug incorporated into the micelles) were estimated for 1.0 g · L^{-1} copolymer solution and are presented in Table 2. Solubilization capacity and encapsulation efficiency can be defined by the following equations:[36]

$$S_{cp} = \frac{(S^{G}_{poly} - S^{G}_{water})}{(C_{poly} - CAC)} \quad (2)$$

$$E_{ef} = \frac{DE}{DA} \times 100 \quad (3)$$

where S^{G}_{poly} is the solubility of griseofulvin in the copolymer solution (mg · L^{-1}), S^{G}_{water} is the solubility of griseofulvin in water (mg · L^{-1}), C_{poly} is the concentration of the copolymer (set to 1.0 g · L^{-1}), DE is the mass of drug

Table 2. Solubility, solubilization capacity, and encapsulation efficiency of griseofulvin for 1.0 g · L^{-1} copolymer solution at different pH.

Copolymer	pH	Solubility[a)]	Solubilization capacity (S_{cp})	Encapsulation efficiency (E_{ef})
		mg · L^{-1}	mg · g^{-1}	%
SAVal-OA(0.16)	5.5	25.3 ± 1.7	15.4 ± 1.7	15.4
	7.4	21.2 ± 3.1	11.5 ± 3.1	11.2
SAVal-DA(0.16)	5.5	37.7 ± 2.6	27.7 ± 2.6	27.7
	7.4	30.6 ± 2.1	20.6 ± 2.1	20.6

[a)]Aqueous solubility of griseofulvin in the absence of polymer is 10 mg · L^{-1} at 25 °C.

encapsulated in the polymer, and DA is the mass of drug added. The solubilization capacity determined at $1.0\,g \cdot L^{-1}$ copolymer in pH = 7.4 buffer solution was $11.5\,mg \cdot g^{-1}$ for SAVal-OA(0.16) and $20.6\,mg \cdot g^{-1}$ for SAVal-DA(0.16). However, the values increased to 15.4 and $27.7\,mg \cdot g^{-1}$, respectively, at pH = 5.5. The solubilization capacities thus obtained were quite large compared with micelle-forming neutral surfactants [e.g., Tween 80 ($3.4\,mg \cdot g^{-1}$), Creomphor EL ($2.6\,mg \cdot g^{-1}$)][37] and triblock copolymers ($\overline{M}_n \approx 5\,000$–$7\,000$) of ethylene oxide and phenyl glycidyl ether (≈4.0–17.8 $mg \cdot g^{-1}$).[38]] This is probably due to the high molecular weight of the copolymer. However, Crothers et al.[39] reported higher solubility of griseofulvin in micellar solutions of block copolymers of polystyrene and PEO or poly(1,2-butylene oxide). As seen in Table 2, copolymer SAVal-OA(0.16) at pH = 7.4 is able to incorporate 11.5% of the drug into its micellar domains, and the value increases up to 15.4% when the solution pH is reduced to 5.5. The encapsulation efficiency further increases to 20.6% and 27.8% by increasing the hydrophobe chain length of the copolymer at pH = 5.5 and 7.4, respectively. Therefore, the copolymers under investigation are quite efficient in increasing the bioavailability of this poorly soluble hydrophobic drug.

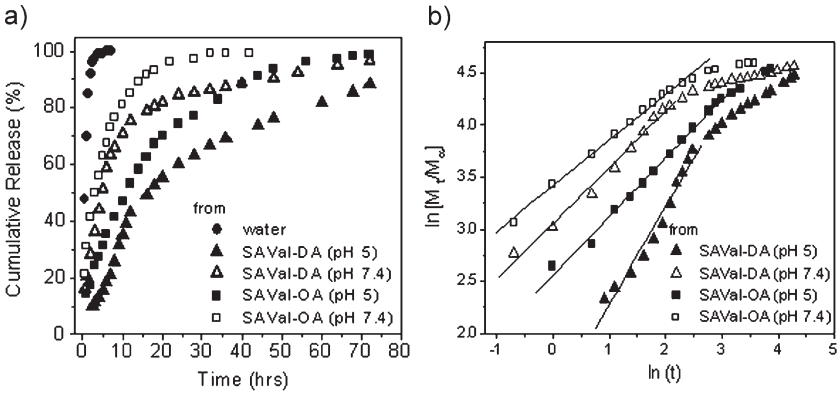

Figure 8. (a) The release profile of griseofulvin from water (●) and from SAVal-OA(0.16) [pH = 5 (■), pH = 7.4 (□)], and SAVal-DA(0.16) [pH = 5 (▲), pH = 7.4 (△)] copolymer micelles with 0.1 M NaCl at 37 °C. (b) Plot of ln $[M_t/M_\infty]$ versus ln t of griseofulvin release at different solution pH.

In vitro Release of Griseofulvin

Dialysis was used to monitor the *in vitro* drug release kinetics. For comparison with the micellar systems, the diffusion of nonencapsulated drug through the dialysis membrane was followed against buffer solution (pH = 5). As seen in Figure 8, almost 100% of the drug diffused through within 3 h, consistent with the expected rate of diffusion for low-molecular-weight drug molecules with no micelles present. To measure the sustaining properties imposed by the polymer, the drug release kinetics were further monitored at pH = 5 and 7.4 for solutions of griseofulvin-loaded copolymer at 37 °C over 72 h. The release profiles thus obtained are presented in Figure 8. In contrast to the rapid release observed for the free drug, the release from the copolymer micelles was slow, corresponding to sustained characteristics. However, an initial burst release was observed in all the cases followed by more gradual release until equilibration was attained over 1–2 days. Furthermore, while roughly 30–40% of the loaded griseofulvin was released in 10 h in pH = 5 solution, the release at pH = 7.4 was much faster and almost 70–80% of the drug escaped through the membrane. Based on this observation, it can be concluded that a large fraction of the drug probably existed at the interstices of the self-assembled nanoparticles causing a burst release, while those located in the interior of the micelles followed slow and stepwise release kinetics. However, at low pH, the polymer micelles were more compact and the rate of drug release became slower.

In order to investigate the mechanism of drug release kinetics, the percentage release of drug was fitted to the power law model according to Equation (4):

$$\frac{M_t}{M_\infty} = kt^n \tag{4}$$

Table 3. Kinetic parameters for release of griseofulvin from copolymer at 37 °C.

Copolymer	pH	Release exponent (n)	Kinetic constant (k)	Correlation coefficient (R^2)
SAVal-OA(0.16)	5	0.56 ± 0.02	12.89 ± 1.03	0.99
	7.4	0.44 ± 0.01	30.26 ± 1.02	0.99
SAVal-DA(0.16)	5	0.94 ± 0.06	3.82 ± 1.12	0.98
	7.4	0.54 ± 0.02	21.2 ± 1.03	0.99

Macromolecular Journals
DOI: 10.1002/mabi.200900135

where k is the release constant and n is the release exponent. Fitting of the experimental data to the above equation for 10–50% release resulted in a correlation coefficient (R^2) of ≈0.98–0.99. The values of kinetic constant (k) and release exponent (n), determined from Figure 8b are presented in Table 3. It is observed that n values vary within the range 0.4–0.9, which suggests that the release of griseofulvin from copolymer nanoparticles follows an anomalous transport mechanism.[40]

Conclusion

Hydrophobically modified poly(*N*-acryloyl-L-valinate) polymers with different hydrophobe chain length produced unicore multipolymer micelles in water above a CAC. With increasing concentration, the average diameter of the micelles was reduced, and compact aggregates were formed. Transmission electron microscopy images revealed the existence of spherical nanoparticles for both copolymers that were tested. The polymer nanoparticles had hydrophobic and viscous microenvironments and were quite effective in encapsulation of the hydrophobic drug, griseofulvin. They were able to encapsulate about 11–20 mg of griseofulvin per gram of copolymer, which could be increased up to ≈15–27 mg by lowering the solution pH to 5. The nanoparticles were sensitive to changes in pH and temperature. This property was successfully utilized for the controlled release of griseofulvin. In contrast to the low-molecular-weight surfactant micelles, slow release of griseofulvin to the surrounding solution (over a period of 72 h) could be achieved from the griseofulvin-loaded polymer nanoparticles at pH = 5. However, the release rates were able to be made faster by increasing the solution pH to 7.4. Such type of polymers would make an interesting drug delivery vehicle. Further work in this direction is being carried out in this laboratory for anticancer and antidepressant drugs.

Acknowledgements: The authors acknowledge the financial support from Basic Research in Nuclear Science (*BRNS*), Department of Atomic Energy (*DAE*) (Grant No. 2006/37/17/BRNS/235), and Ministry of Human Resource Development (*MHRD*). P. D. thanks the Council of Scientific and Industrial Research (*CSIR*) [09/081(0519)/2005-EMR-I] for a research fellowship. The authors are thankful to Dr. *N. Sarkar*, Department of Chemistry, Indian Institute of Technology, Kharagpur, for assistance with DLS measurements.

Received: April 6, 2009; Revised: May 17, 2009; Accepted: May 18, 2009; Published online: August 14, 2009; DOI: 10.1002/mabi.200900135

Keywords: amphiphilic polymer nanoparticles; drug solubilization; dynamic light scattering; fluorescence; release kinetics

[1] D. Thompson, M. V. Chaubal, *Drug Deliv. Technol.* **2000**, *2*, 34.
[2] H. Müller, "*Colloidal Carriers for Controlled Drug Delivery and Targeting: Modification, Characterization, and In Vivo Distribution*", Wissenschaftliche Verlagsgesellschaft, Stuttgart 1991.
[3] S. Cohen, H. Bernstein, "*Microparticulate Systems for the Delivery of Proteins and Vaccines*", Marcel Dekker, New York 1996.
[4] G. R. Newkome, C. N. Moorefield, G. R. Baker, M. J. Saunders, S. H. Grossman, *Angew. Chem. Int. Ed. Engl.* **1991**, *30*, 1178.
[5] F. Quirion, S. St-Pierre, *Biophys. Chem.* **1991**, *40*, 129.
[6] I. R. Schmolka, "Poloxamers in the Pharmaceutical Industry", in: *Polymers for Controlled Drug Delivery*, P. J. Tarcha, Ed., CRC Press, Boca Raton 1991.
[7] T. P. Johnston, S. C. Miller, *J. Parenter. Sci. Technol.* **1985**, *39*, 83.
[8] A. V. Kabanov, V. P. Chekhonin, V. Alakhov, E. V. Betrakova, A. S. Lebedev, N. S. Mellik-Nubarov, S. A. Arzakov, A. V. Levashov, G. V. Morozov, E. S. Severin, V. A. Kabanov, *FEBS Lett.* **1989**, *258*, 343.
[9] S. Lin, Y. Kawashima, *Pharm. Acta Helv.* **1985**, *60*, 345.
[10] V. Batrakova, T. Y. Dorodnich, E. Y. Klinskii, E. N. Kliushnenkova, O. B. Shemchukova, O. N. Goncharova, V. Y. Arjakov, V. Alakhov, A. V. Kabanov, *Br. J. Cancer* **1996**, *74*, 1545.
[11] D. Forster, C. Washington, S. S. Davis, *J. Pharm. Pharmacol.* **1988**, *40*, 325.
[12] G. Gaucher, M. Dufresne, V. P. Sant, N. Kang, D. Maysinger, J. Leroux, *J. Controlled Release* **2005**, *109*, 169.
[13] K. Kataoka, A. Harada, Y. Nagasaki, *Adv. Drug Delivery Rev.* **2001**, *47*, 113.
[14] N. Kumar, M. N. V. Ravikumar, A. J. Domb, *Adv. Drug Delivery Rev.* **2001**, *53*, 23.
[15] Y. Hu, G. L. Smith, M. F. Richardson, C. L. McCormick, *Macromolecules* **1997**, *30*, 3526.
[16] Y. Morishima, S. Nomura, T. Ikeda, M. Seki, M. Kamachi, *Macromolecules* **1995**, *28*, 2874.
[17] S. Yusa, M. Kamachi, Y. Morishima, *Langmuir* **1998**, *14*, 6059.
[18] T. Noda, Y. Morishima, *Macromolecules* **1999**, *32*, 4631.
[19] Y. Sato, A. Hashidzume, Y. Morishima, *Macromolecules* **2001**, *34*, 6121.
[20] A. F. Olea, R. G. Barraza, I. Fuentes, B. Acevedo, F. Martinez, *Macromolecules* **2002**, *35*, 1049.
[21] R. G. Barraza, A. F. Olea, C. E. Valdebenito, V. Dougnac, I. J. Fuentes, *J. Colloid Interface Sci.* **2004**, *275*, 434.
[22] Y. Tan, C. Liu, *Colloids Surf. B* **2009**, *69*, 178.
[23] G. B. Jiang, D. Quan, K. Liao, H. Wang, *Mol. Pharm.* **2006**, *3*, 152.
[24] P. Dutta, J. Dey, G. Ghosh, R. R. Nayak, *Polymer* **2009**, *50*, 1516.
[25] A. Bentolila, I. Vlodavsky, R. Ishai-Michaeli, O. Kovalchuk, C. Haloun, A. J. Domb, *J. Med. Chem.* **2000**, *43*, 2591.
[26] M. E. N. Pinho, F. M. L. L. Costa, F. B. S. Filho, N. M. P. S. Ricardo, S. G. Yeates, D. Attwood, C. Booth, *Int. J. Pharm.* **2007**, *328*, 95.
[27] T. Kawata, A. Hashidzume, T. Sato, *Macromolecules* **2007**, *40*, 1174.
[28] A. Mohanty, T. Patra, J. Dey, *J. Phys. Chem. B* **2007**, *111*, 7155.
[29] A. Nakajima, *J. Mol. Spectrosc.* **1976**, *61*, 467.
[30] S. Roy, A. Mohanty, J. Dey, *Chem. Phys. Lett.* **2005**, *414*, 23.
[31] J. Zipfel, J. Berghausen, G. Schmidt, P. Lindner, P. Alexandridis, W. Richtering, *Macromolecules* **2002**, *35*, 4064.

[32] M. L. Bennett, A. B. Fleischer, J. W. Loveless, S. R. Feldman, *Pediatr. Dermatol.* **2000**, *17*, 304.
[33] W. L. Chiou, S. Riegelman, *J. Pharm. Sci.* **1971**, *60*, 1376.
[34] M. S. Sue, K. M. Liu, H. S. Yu, *Yi Xue Ke Xue Za Zhi Gaoxiong* (Medline) **1993**, *9*, 1.
[35] K. M. Tur, H. S. Ch'ng, S. Baie, *Int. J. Pharm.* **1997**, *148*, 63.
[36] [36a] S. H. Yalkowsky, *"Solubility and Solubilization in Aqueous Media"*, Oxford University Press, New York 1999, Chapter 7; [36b] V. S. Miguel, A. J. Limer, D. M. Haddleton, F. Catalina, C. Peinado, *Eur. Polym. J.* **2008**, *44*, 3853.
[37] B. D. Balakrishnan, G. L. Rege, J. E. Amidon, *J. Pharm. Sci.* **2004**, *93*, 2064.
[38] P. Taboada, G. Velasquez, S. Barbosa, V. Castelletto, S. K. Nixon, Z. Yang, F. Heatley, I. W. Hamley, M. Ashford, V. Mosquera, D. Attwood, C. Booth, *Langmuir* **2005**, *21*, 5263.
[39] M. Crothers, Z. Zhou, N. M. P. S. Ricardo, Z. Yang, P. Taboada, C. Chaibundit, D. Attwood, C. Booth, *Int. J. Pharm.* **2005**, *293*, 91.
[40] P. L. Ritger, N. A. Peppas, *J. Controlled Release* **1987**, *5*, 23.

DOI: 10.1002/mabi.200900135